STEM CELLS TRANSLATIONAL MEDICINE®

ENABLING TECHNOLOGIES FOR CELL-BASED CLINICAL TRANSLATION

Genome Editing in Neuroepithelial Stem Cells to Generate Human Neurons with High Adenosine-Releasing Capacity

DANIEL POPPE,[a] JONAS DOERR,[a] MARION SCHNEIDER,[b] RUVEN WILKENS,[a] JULIUS A. STEINBECK,[a] JULIA LADEWIG,[a,d,e,f] ALLISON TAM,[c] DAVID E. PASCHON,[c] PHILIP D. GREGORY,[c] ANDREAS REIK,[c] CHRISTA E. MÜLLER,[b] PHILIPP KOCH,[a,d,e,f] OLIVER BRÜSTLE[a]

Key Words. Adenosine secretion • Gene-editing • Human neurons • Adenosine kinase • Neuroepithelial stem cells

ABSTRACT

As a powerful regulator of cellular homeostasis and metabolism, adenosine is involved in diverse neurological processes including pain, cognition, and memory. Altered adenosine homeostasis has also been associated with several diseases such as depression, schizophrenia, or epilepsy. Based on its protective properties, adenosine has been considered as a potential therapeutic agent for various brain disorders. Since systemic application of adenosine is hampered by serious side effects such as vasodilatation and cardiac suppression, recent studies aim at improving local delivery by depots, pumps, or cell-based applications. Here, we report on the characterization of adenosine-releasing human embryonic stem cell-derived neuroepithelial stem cells (long-term self-renewing neuroepithelial stem [lt-NES] cells) generated by zinc finger nuclease (ZFN)-mediated knockout of the adenosine kinase (ADK) gene. ADK-deficient lt-NES cells and their differentiated neuronal and astroglial progeny exhibit substantially elevated release of adenosine compared to control cells. Importantly, extensive adenosine release could be triggered by excitation of differentiated neuronal cultures, suggesting a potential activity-dependent regulation of adenosine supply. Thus, ZFN-modified neural stem cells might serve as a useful vehicle for the activity-dependent local therapeutic delivery of adenosine into the central nervous system. STEM CELLS TRANSLATIONAL MEDICINE *2018;7:477–486*

SIGNIFICANCE STATEMENT

This study generated human neuroepithelial stem cell (long-term self-renewing neuroepithelial stem cells) deficient for adenosine kinase (ADK), the most important cellular metabolizing enzyme of adenosine. The purine nucleoside adenosine has been described to have extensive neuroprotective properties under various pathological conditions of the brain and can counteract overshooting neuronal activity. The resulting cells can be efficiently differentiated into neurons and astrocytes in vitro and in vivo and exhibit elevated adenosine releasing capacities. Secretion of adenosine from neurons can be triggered by excitation, providing the basis for ADK-deficient neurons as an attractive therapeutic tool for the local "on-demand" delivery in epilepsy.

INTRODUCTION

The purine nucleoside adenosine has essential roles in many biochemical processes of the human body such as energy homeostasis or signal transduction. Under stress conditions, adenosine is upregulated, a response that can have extensive protective effects in various organs, including the cardiovascular, gastrointestinal, renal, muscular, or immune system [1–3]. In the central nervous system (CNS), high neuronal activity elicits an increase in adenosine release, which acts via A_1 receptors inhibiting the release probability of presynaptic glutamate and activating postsynaptic G protein-coupled inwardly rectifying potassium (GIRK) channels, thereby eliciting postsynaptic hyperpolarization [4, 5]. These responses attenuate excessive neuronal activity, thereby protecting against several pathological conditions such as ischemic injuries, trauma, reduced oxygen supply, pain, and in particular, epileptic seizures [6, 7]. In this context, adenosine and pharmacological activators of its neuronal A_1 receptors have been shown to act as potent anticonvulsant drugs [8].

Due to these broad neuroprotective properties, adenosine has been considered as a potential

[a]Institute of Reconstructive Neurobiology, University of Bonn and Hertie Foundation, Bonn, Germany; [b]PharmaCenter Bonn, Pharmaceutical Institute, Pharmaceutical Chemistry I, University of Bonn, Bonn, Germany; [c]Sangamo Therapeutics, Richmond, California, USA; [d]Central Institute of Mental Health, University of Heidelberg/ Medical Faculty Mannheim, Mannheim, Germany; [e]Hector Institute for Translational Brain Research (HITBR gGmbH), Mannheim, Germany; [f]German Cancer Research Center (DKFZ), Heidelberg, Germany

Correspondence: Oliver Brüstle, M.D., Institute of Reconstructive Neurobiology, Life & Brain Center, University of Bonn, Medical Faculty, Sigmund-Freud-Str. 25, Bonn 53127, Germany. Telephone: +49 (0)228 6885 500; e-mail: brustle@uni-bonn.de; or Philipp Koch, M.D., Hector Institute for Translational Brain Research (HITBR), Central Institute of Mental Health, University of Heidelberg, Medical Faculty Mannheim, J5, Mannheim 68159, Germany. Telephone: (+49) 621 1703 6711; e-mail: philipp.koch@zi-mannheim.de

Received June 6, 2016; accepted for publication January 29, 2018; first published March 28, 2018.

http://dx.doi.org/10.1002/sctm.16-0272

therapeutic agent to treat disorders of the CNS. However, hampered by its diverse systemic actions such as cardiac suppression or vasodilation [9], its fast-metabolic breakdown and an insufficient permeability of the blood-brain-barrier [10], delivery of adenosine to the CNS has remained challenging. In attempts to bypass this limitation, adenosine has been delivered locally using mini-pumps or cell free deposits of silk-polymers. These experiments revealed temporary but potent anticonvulsive modulation of epileptic activity in a kindling model of epileptogenesis [11, 12].

Adenosine is mostly metabolized by two enzymes, adenosine deaminase (ADA) and adenosine kinase (ADK), the latter being more efficient with a k_m value of 1 μM compared to 100 μM for ADA [13]. Based on these metabolizing pathways, the concept of generating cell populations deficient in ADK was developed for cell-mediated adenosine delivery [14]. In this model, increased intracellular adenosine levels result in a release of adenosine from ADK-deficient cell populations, most likely via equilibrative diffusion transporters which are widely expressed in the CNS [15–17] (Supporting Information Fig. S1).

Indeed, knockdown or knockout of *ADK* has been shown to result in cell populations with potent neuroprotective properties. ADK deficient myoblasts or fibroblasts transplanted in encapsulated polymer membranes were able to temporarily protect animals from seizures in a rat kindling model [18, 19]. In the human system, small interfering RNA(siRNA)-mediated knockdown of *ADK* in mesenchymal stem cells resulted in an 80% decrease in enzymatic activity, leading to decreased seizure events in the mouse kainate acid model by 35% [20]. Non-neural cells, which have to be encapsulated, elicit their effects via a passive paracrine and non-activity dependent mode of action and show only limited survival times. In contrast, adenosine release from neural cells integrated into the CNS might allow long-term supply of adenosine. In the case of neurons functionally integrated into epileptic neuronal networks, an activity-dependent release might serve as a potent source of adenosine "on demand" in epileptic tissue. In line with this idea, we have explored neural progenitors derived from $ADK^{-/-}$ murine embryonic stem cells. Following transplantation into a murine kindling model of epileptogenesis, transplanted cells significantly delayed epileptogenesis and were superior to non-neuronal BHK-AK2 hamster kidney cells [21].

With the advent of human pluripotent stem cells such as human embryonic stem cells (hESCs) or induced pluripotent stem cells (iPSCs), human cell populations are now available, which can be efficiently differentiated into neural progenitors and their progeny. In this context, we have recently described a population of hESC-derived long-term self-renewing neuroepithelial stem cells (lt-NES) [22, 23]. Similar to pluripotent stem cells, this population exhibits strong self-renewal capacity enabling genetic modification, subsequent clonal selection and expansion at a scale sufficient for potential therapy. Independent of the passage number, these cells consistently give rise to functional neurons [22–24]. Furthermore, they can be guided towards specific neuronal or glial cell populations [22]. Importantly, lt-NES cell-derived transplants exhibit excellent long-term survival and functional, synaptic integration into the hosts' brain without the risk of teratoma formation or neural overgrowth [22, 25]. Taken together, these properties make lt-NES cells an attractive candidate population for gene targeting of the *ADK* locus and potential future cell-based therapies.

Here, we describe that zinc finger nucleases (ZFNs-) mediated gene disruption can be directly applied to lt-NES cells to generate ADK-deficient human neural cells. $ADK^{-/-}$ lt-NES cells and their differentiated neuronal and glial progeny show a pronounced increase of adenosine release. Importantly, we report that adenosine release in $ADK^{-/-}$ neurons can be triggered by excitation, a property which could be particularly attractive for future cellular therapy exploiting activity-dependent adenosine release from grafted engineered cells to locally counteract hyperexcitation.

Materials and Methods

Cell Culture

lt-NES cells derived from the hESC line I3 have been generated previously [22]. The cells were cultured in N2 media: Dulbecco's Modified Eagle Medium (DMEM)/F12 + 1% N2-supplement (all Life Technologies, Darmstadt, Germany) + 1,6 mg/l D-Glucose (Sigma-Aldrich, Steinheim, Germany), supplemented with B27 supplement (1:1,000, Life Technologies), epidermal growth factor(EGF) and basic fibroblast growth factor(FGF2) (10 ng/ml each; R&D Systems, Minneapolis, MN). Cells were passaged every 3–4 days using trypsin, by plating 500,000 cells per 3.5 cm well. For terminal differentiation, lt-NES cells were transferred to Geltrex (Life Technologies)-coated cell culture dishes. Upon reaching 100% confluence, culture medium was changed to differentiation medium (50% N2 media + 50% Neurobasal media [Life Technologies] + 2% B27 Supplement [Life Technologies] + 10 mM cAMP [Sigma-Aldrich]), which was exchanged every other day. To generate astrocyte-enriched cultures, differentiation media was supplemented with 10% fetal calf serum (FCS, Life Technologies) from week 2 to 5 before switching back to FCS-free medium, while neuronal enrichment was achieved by adding 5 μM N-[N-(3,5-Difluorophenacetyl)-L-alanyl]-S-phenylglycine t-butyl ester (DAPT, Sigma-Aldrich) for the first 5 days of culture. Cell viability was determined with PrestoBlue reagent (Life Technologies) according to the manufacturer's instructions. For the determination of growth rates, defined numbers of lt-NES cells (100,000 cells/cm^2) were plated at the beginning of each passage, and total cell numbers were counted 3 days later before plating, again, 100,000 cells/cm^2 on fresh tissue culture dishes to start a new passage. Cell numbers were cumulated along passage count taking the cell numbers at the beginning and the end of each passage into account.

Generation of ADK Knockout lt-NES Cells

Plasmids coding for zinc fingers binding upstream and downstream of the desired cleavage site were generated by Sangamo Therapeutics. ZFNs targeting the *ADK* gene were designed by modular assembly using an archive of one- and two-finger modules and optimized for binding essentially as previously described [26]. ZFN-encoding plasmids were introduced into lt-NES cells by nucleofection (program B23; Lonza, Basel, Switzerland) using 1 μg of each plasmid and 1 × 10^6 lt-NES cells. Seven days after nucleofection, chemoselection with 10 μM 8-Cl-cAMP (8-chloro-adenosine 3′,5′-cyclic monophosphate; Enzo) and 10 μM 8-Cl-Ado (8-chloro-adenosine; Enzo Life Science, Lorrach, Germany) was applied for 3 weeks. Emerging clones were manually picked and expanded for sequencing. Sequencing products were generated from genomic DNA using the following primer pair: GGGTTCCTGCGGCCGCCGTTTCTGCTTTTTAAAGCTCATGT and TATGG ATCCACTAGTTA TGTAAATACAAAC ACAGAAAACCAA.

Single Nucleotide Polymorphism Karyotyping

Genomic DNA was prepared using the DNeasy Blood & Tissue Kit according to manufacturer's instructions (Qiagen, Hilden, Germany). Whole-genome single nucleotide polymorphism (SNP) genotyping was performed at the Institute of Human Genetics at the University of Bonn, Germany. Genomic DNA at a concentration of 50 ng/μl was used for whole-genome amplification. Afterward, the amplified DNA was fragmented and hybridized to sequence-specific oligomers bound to beads on an Illumina HumanOmniExpress BeadChip 12V1.0 chip (Illumina, San Diego, CA). Data were analyzed using Illumina GenomeStudio V2011.1 with the cnvPartition 3.2.0 plugin.

Immunocytochemical Analysis

Cells were fixed in 4% paraformaldehyde (PFA) for 15 minutes at room temperature (RT), washed twice in phosphate-buffered saline (PBS) and blocked with 10% FCS and 0.1% Triton-X-100 in PBS (blocking solution) for 30 minutes at RT. Primary antibodies (beta III-tubulin: Biolegend (San Diego, CA) PRB-435P, 1:1,000; DACH1: Proteintech (Rosemont, IL) 10914-1-AP, 1:500; glial fibrillary acidic protein (GFAP): Agilent (Santa Clara, CA) ZO334, 1:500; MAP2ab: Sigma-Aldrich M1406, 1:1,000; Nestin: R&D Systems MAB1259, 1:500; PLZF: EMD Millipore (Billerica, MA) OP128, 1:50; Sox2: R&D Systems MAB 2018, 1:500; ZO-1: Life Technologies 61–7300, 1:100) were applied overnight at 4°C in blocking solution. Cells were washed twice with PBS before secondary antibodies (Alexa488 anti-ms, Alexa555 anti-ms, Alexa488 anti-rb, and Alexa555 anti-rb; all 1:1,000, Life Technologies) were applied for 2 hours in blocking solution at RT. Cell nuclei were counterstained with 4',6-diamidino-2-phenylindole (DAPI), and specimens were mounted with Mowiol. Numbers of different cell types were quantified by counting at least 1,000 cells in randomly picked fields (two independent experiments) at ×400 magnification. Nuclei stained with DAPI were correlated to the perinuclear staining for the cell type-specific markers.

Western Immunoblotting

Cells were harvested in RIPA buffer (1 hour; 4°C; Sigma-Aldrich) containing protease inhibitors (cOmplete ULTRA [Roche, Basel, Switzerland]). Lysates were clarified by centrifugation (10,000*g*, 15 minutes, 4°C) and run on a sodium dodecyl sulfate polyacrylamide gel electrophoresis (SDS-PAGE) using standard gels (10%). Separated proteins were blotted on MeOH-activated polyvinylidene difluoride (PVDF) membranes, blocked with 10% Roti-Block (Carl Roth, Karlsruhe, Germany) in tris-buffered saline with Tween-20 (TBST) for 20 minutes and incubated with primary antibodies rabbit anti-ADK (Abcam [Cambridge, United Kingdom] ab204430; 1:50) and mouse anti-actin (EMD Millipore MAB 1501; 1:5,000) overnight at 4°C. Membranes were washed, incubated with an horseradish peroxidase (HRP)-linked secondary antibody (Thermo Fisher Scientific (Waltham, MA) Goat anti-mouse Poly-HRP, 1:1,000) for 1 hour and visualized by chemoluminescence (Thermo Fisher Scientific SuperSignal West Dura Chemiluminescent Substrate).

Transplantation Experiments and Immunohistochemistry

RAG2-deficient mice of C57BL/6 background were used at an age of 8–10 weeks (body weight 22–28 g) for stereotaxic transplantation of lt-NES cells. Animals were monitored for wound infections and neurological deficits on a daily basis during the first 2 weeks after transplantation and in weekly intervals thereafter. Animals were sacrificed 16 weeks after transplantation and transcardially perfused. Fixed brains were frozen and cut into 40 μm sections for analysis. For immunohistochemistry, primary antibodies (rat anti-Neurofilament-M/HO14, a gift from Virginia Lee, 1:20; mouse anti-human-specific synaptophysin, Stressmarq, [Victoria, Canada] SMC-178, 1:500) were applied overnight at 4°C in blocking solution containing 10% FCS (Life Technologies) and 0.2% Triton in PBS. Cells were washed twice in PBS before secondary antibodies (Alexa488 anti-mouse, Alexa555 anti-rat; all 1:1,000, Life Technologies) were applied for 2 hours at RT in blocking solution. Cell nuclei were counterstained with DAPI, the specimens were mounted with Mowiol. HO14-positive neurofilaments and synaptophysin-positive punctae were quantified using the ImageJ software in 10 μm thick confocal stacks using the "Analyze Particle" function with a minimal cutoff size of 0.2 (square inch) and the "Ridge Detection" plugin (sigma 1.51; lower threshold 3.06; upper threshold 7.99), respectively. Based on these data, the coverage of synaptophysin-positive punctae per 10 μm neurofilaments was calculated. Significance was determined using unpaired *t* test, $p = .6705$, ns.

Ethical Statement

All animal procedures were performed in agreement with the European Union and German guidelines and were approved by the Government of North Rhine-Westphalia (permit number: AZ 8.87-51.04.20.09.354).

Reverse Transcriptase-PCR Analysis

Cellular RNA was extracted using the RNeasy kit (Qiagen), and cDNA was generated using the iScript cDNA synthesis kit (Bio-Rad, Hercules, CA). Reverse transcription polymerase chain reaction (RT-PCR) was performed using TaqDNA Polymerase (Life Technologies). Quantitative real-time RT-PCR reactions were performed with miScript SYBR Green PCR Kit (Qiagen) on an Eppendorf (Hamburg, Germany) Mastercycler. Primers were: Reference gene *RPLP0* (AGCCCAGAACACTGGTCTC; ACTCAGGATTTCAATGGTGCC), *ADA* (GCCTTCGACAAGCCCAAAGTA; CTCTGCTGTGTTAGCTGGGAG), *ADK* (CAGAAGCTGCCACTTTTGCT; GAGTTCATCTTTGGCAGGGC). Data were normalized to RPLP0 levels and human fetal brain RNA (Agilent). PCR products were assessed by dissociation curve and gel electrophoresis, and normalized data were analyzed using the ΔΔCt method.

Quantitative Measurement of Adenosine

Adenosine levels were measured using high-pressure liquid chromatography (HPLC) coupled to mass spectrometry (MS). Media was removed from the cells, cells were washed twice in PBS, and cell buffer was added (140 mM NaCl, 4 mM KCl, 1.8 mM $CaCl_2$, 2.2 mM $MgSO_4$, 0.48 mM NaH_2PO_4, 2 mM sodium pyruvate, 5.5 mM D(+)-glucose, 10 mM HEPES, pH 7.4, complemented with 100 μM of the ADA-inhibitor erythro-9-2-hydroxy-3-nonyl-adenine [EHNA, Sigma-Aldrich]). Supernatants were collected at indicated time points and subsequently lyophilized. The residues were dissolved in methanol with 1% acetic acid using sonication. After precipitation of inorganic salts by centrifugation for 1 hour at 10,000*g*, supernatants were directly used for HPLC-MS analysis. Samples (5 μl) were injected at a flow rate of 0.3 ml/minute into a HPLC Dionex Ultimate 3000 system (Thermo Fisher Scientific) coupled to a micrOTOF-Q mass spectrometer (Bruker, Billerica,

MA) with an electrospray ionization source. Chromatographic separation was performed on a SYNERGI 4 u POLAR-RP column (a hydrophobic ether-bonded phenyl-phase column, Phenomenex, Torrance, CA) at 25°C. It was started with 100% H_2O containing 0.1% acetic acid followed by a gradient for 4 minutes to 100% acetonitrile containing 0.1% acetic acid, which was started after 2.5 minutes. The column was flushed for further 6.5 minutes with 100% acetonitrile containing 0.1% acetic acid. Positive scan MS was observed from 50 to 1,000 m/z optimized to peak 268.1038. For quantification, the extract ion counts 268.1038 ± 0.01 was used. Calibration curves were determined by dissolution of a broad range of adenosine concentrations in (a) acetonitrile: water (1:1), and (b) in the matrix (cell supernatant). The limit of detection (LOD) of the method was below 1 ng/ml for adenosine dissolved in the acetonitrile-water mixture. In the matrix, the LOD was about 10-fold higher (approximately 10 ng/ml).

Glutamatergic Stimulation Experiments

Upon removal of the culture medium cells were washed twice in PBS, and cell buffer containing 100 μM EHNA and 100 μM glycine (both Sigma-Aldrich) was added. After 1 and 8 hours, 100 μM glutamate (Sigma-Aldrich), 100 μM N-Methyl-D-aspartate (NMDA), or 100 μM α-amino-3-hydroxy-5-methyl-4-isoxazolepropionic acid (AMPA) (both Tocris, Bristol, United Kingdom) was applied to the supernatant, which was collected after a total time of 24 hours and subjected to HPLC analysis as described above. D-2-amino-5-phosphonovalerate (D-APV) (50 μM) and NBQX (10 μM; both Tocris) were applied 30 minutes before first glutamate treatment where indicated.

Statistical Analyses

Quantitative PCR analyses were performed in two independent experiments run as triplicates. Cell viability assays were performed in triplicates. Measurement of adenosine release was performed from three independent biological replicates. The data are presented as mean + SD. Statistical significance was analyzed by two-tailed Student's *t* test.

Results

Generation of Genetically Engineered ADK$^{-/-}$ Pluripotent Stem Cell-Derived Neural Stem Cells

As a starting population, we used lt-NES cells previously established from the hESC line I3 [22]. During proliferation, these cells form rosette-like structures and homogeneously express the neural stem cells markers NESTIN, SOX2 as well as the rosette-associated markers PLZF and DACH1. As a correlate of their epithelial nature, the zonula occludens protein 1 (ZO-1) is located at the luminal, apical part of the rosette-like structures (Fig. 1A). Upon growth factor withdrawal, lt-NES cells differentiate into a major fraction of beta III-tubulin- and MAP2ab-positive neurons and a minor fraction of GFAP-positive astrocytes (Fig. 1A), a differentiation potential, which remains stable for at least 70 passages in vitro [22]. In a first set of experiments, we investigated expression levels of ADK in proliferating lt-NES cells as well as following growth factor withdrawal for 6 weeks using quantitative RT-PCR. As reference, cDNA from commercial fetal brain RNA probes was included in the study. Even though expression levels were lower than in the reference probes (which consist of a mixture of neurons, progenitors and non-neural cells), we detected distinct expression of the transcript in lt-NES cells, which was increased following differentiation (Fig. 1B). Together with the stability of lt-NES cells, the expression data qualify these cells for gene targeting of the *ADK* locus. For genetic disruption of the *ADK* locus, we used ZFN-mediated targeted gene disruption. Synthetic fusion proteins of a FokI nuclease domain and a zinc-finger-type DNA-binding domain were designed to target exon 5 of the *ADK* gene, upstream of the essential catalytic domain of the *ADK* gene located in exon 10. The ZFNs are used in pairs, with one ZFN binding directly upstream of the intended cleavage site, the other one downstream of it. After binding, the close proximity of their nuclease domains leads to their dimerization and consequent activation of double strand break-inducing activity. The cellular machinery for nonhomologous end joining is involved in repairing the double strand break [27], but this mechanism is error-prone and thus can result in disruption of the target gene by for instance frame shift mutations (Fig. 1C). In case of the *ADK* locus, selection for successful targeting and disruption of the gene can be achieved by administration of 8-chloro-adenosine and 8-chloro-cAMP, which are converted to cytotoxic metabolites by functional ADK [28].

ZFNs were introduced into lt-NES cells by plasmid nucleofection [29], and selection was initiated 6 days later. Single clones surviving the selection process were manually picked and expanded for further characterization. No clones were obtained when selection was performed on untreated cells. Genomic sequencing revealed a homozygous deletion of tyrosine at position 165 of exon 5 in more than 80% of a total of 148 analyzed clones (Fig. 1D). This one base pair deletion results in a frame shift and the premature disruption of translation due to a new stop codon located at amino acid position 162 (Fig. 1E). At lower frequencies, we observed frame shift-causing deletions of 7 bp (4%) and 8 bp (3.4%; Supporting Information Fig. S2). Remarkably, the vast majority of derived clones (>90%) showed a homozygous sequence alteration of both alleles. The remaining clones showed either heterozygous alterations as seen by superimposed sequencing signals starting at the position of the ZFN cleavage or the monoallelic integration of large fractions of plasmid DNA pieces as seen by long PCR amplificates (Supporting Information Fig. S2). As the application of gene targeting by nucleases and clonal selection of human cell populations might result in karyotypic abnormalities, we assessed the karyotypic integrity of our ADK$^{-/-}$ lt-NES cell lines using high-resolution SNP-based genotyping (Supporting Information Fig. S3); lines displaying karyotypic abnormalities were excluded from the study. ADK$^{-/-}$ lt-NES cells were indistinguishable from wild-type lt-NES cells with respect to their morphology and marker expression during proliferation and upon withdrawal of the growth factors. Comparable to wild-type lt-NES cells, they exhibited expression of NESTIN, SOX2, PLZF, DACH1 as well as polarized expression of ZO-1 (Fig. 2A). Importantly, Western blot analysis confirmed the absence of wild-type ADK in targeted ADK$^{-/-}$ lt-NES cells (Fig. 2B).

To analyze ADK$^{-/-}$ lt-NES cells in more detail, we investigated growth rates of ADK$^{-/-}$ cells in comparison to their parental wild-type lt-NES cells and observed no significant differences both at early and later passages (Supporting Information Fig. S4). In addition, we quantified the proportion of immunolabeled neurons (beta III-tubulin and MAP2ab) and astrocytes (GFAP) in ADK$^{-/-}$ and wild-type cells following a 4-week growth factor withdrawal. This analysis revealed no significant differences in the differentiation potential of both populations (Fig. 2C). We further assessed whether ADK-deficiency might interfere with the cells' ability to

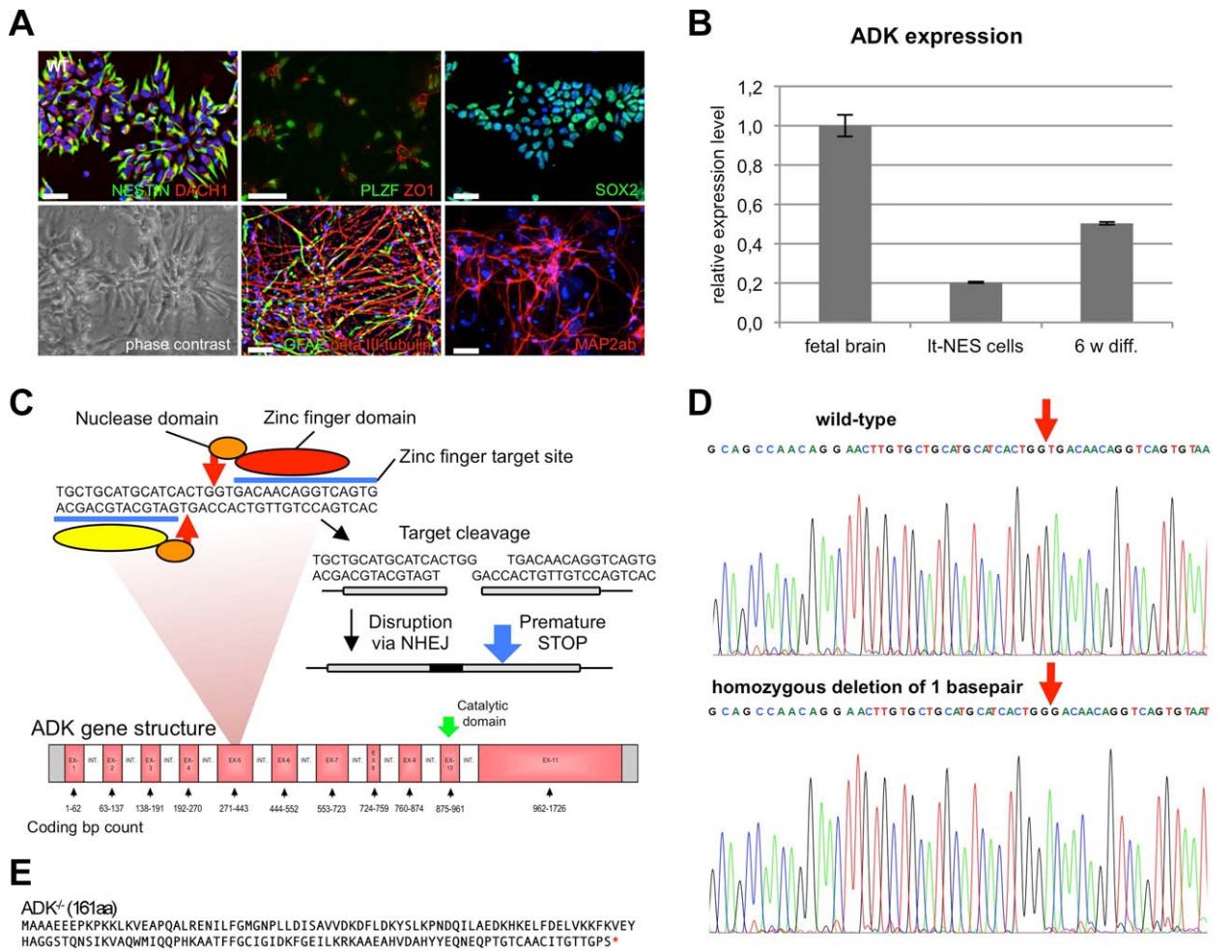

Figure 1. Generation of ADK-deficient neural stem cells. **(A):** Long-term self-renewing neuroepithelial stem cells (lt-NES cells) stably proliferate in the presence of the growth factors FGF2 and EGF and show rosette-like morphology with expression of NESTIN, PLZF, and SOX2 as well as polarized expression of the tight junction marker ZO-1. Following growth factor withdrawal, lt-NES cells differentiate into a major fraction of beta III-tubulin- and MAP2ab-positive neurons and a minor fraction of GFAP-positive astrocytes. **(B):** Quantitative PCR analysis of adenosine kinase (ADK) in lt-NES cells and their differentiated progeny, normalized to RPLP0 as housekeeping gene and compared to ADK expression in human fetal brain RNA. **(C):** Cartoon demonstrating the zinc finger nuclease gene disruption strategy in exon 5 of the *ADK* gene. A pair of zinc finger nucleases induces a targeted double strand break (red arrows) after binding to their target site (indicated by blue lines). Repair via nonhomologous-end-joining can drive a frame shift resulting in premature disruption of translation (blue arrow). The catalytic core around Asp316 is situated in exon 10 (of 11) at the C-terminal end of the protein. Introduction of frame shifts in front of the catalytic part leads to elimination of all enzymatic activity. **(D):** Sequencing of the target locus revealed a homozygous deletion of 1 bp (thymidine 165 of exon 5) in 81.7% of the 148 analyzed clones (red arrow). **(E):** This frame shift leads to a stop codon (asterisk) after 161 translated amino acids, resulting in a complete loss of ADK activity. Scale bars: 50 μm. Abbreviations: ADK, adenosine kinase; EGF, epidermal growth factor; FGF2, basic fibroblast growth factor; GFAP, glial fibrillary acidic protein; lt-NES cell, long-term self-renewing neuroepithelial stem cell; PCR, polymerase chain reaction.

differentiate into neurons and express synaptic markers in vivo. To that end, we transplanted both populations into immunodeficient mice and analyzed the transplants 16 weeks later. We found that both populations differentiated into large numbers of neurons detected by a human specific marker to neurofilament. In addition, we detected prominent expression of synaptophysin, indicating that lack of ADK does not interfere with the cells' principal ability to differentiate into neurons expressing proteins required for synapse formation in vivo (Fig. 2D and Supporting Information Fig. S5). Importantly, the density of synaptophysin-positive punctae along neurofilament-positive fibers was found to be very similar in both, WT and $ADK^{-/-}$ neuron populations (Fig. 2D). Established $ADK^{-/-}$ lt-NES cells lines further exhibited robust resistance to continuous administration of 8-Cl-adenosine at concentrations toxic to wild-type cells, thereby providing additional biochemical evidence for the lack of ADK enzymatic activity (Fig. 2E). Thus, wild-type and genome-edited $ADK^{-/-}$ lt-NES cells are indistinguishable with respect to their growth and differentiation properties.

ADK-Deficient Neural Stem Cells and Their Differentiated Progeny Release Elevated Levels of Adenosine

We next investigated whether the disruption of the *ADK* locus results in increased levels of secreted adenosine in the supernatant of proliferating and differentiated $ADK^{-/-}$ cells compared to wild-type controls using liquid chromatography tandem mass spectrometry (LC-MS/MS; all experiments were performed in controlled detection buffer, see "Materials and Methods" section). This analysis revealed a significant increase in $ADK^{-/-}$ cells

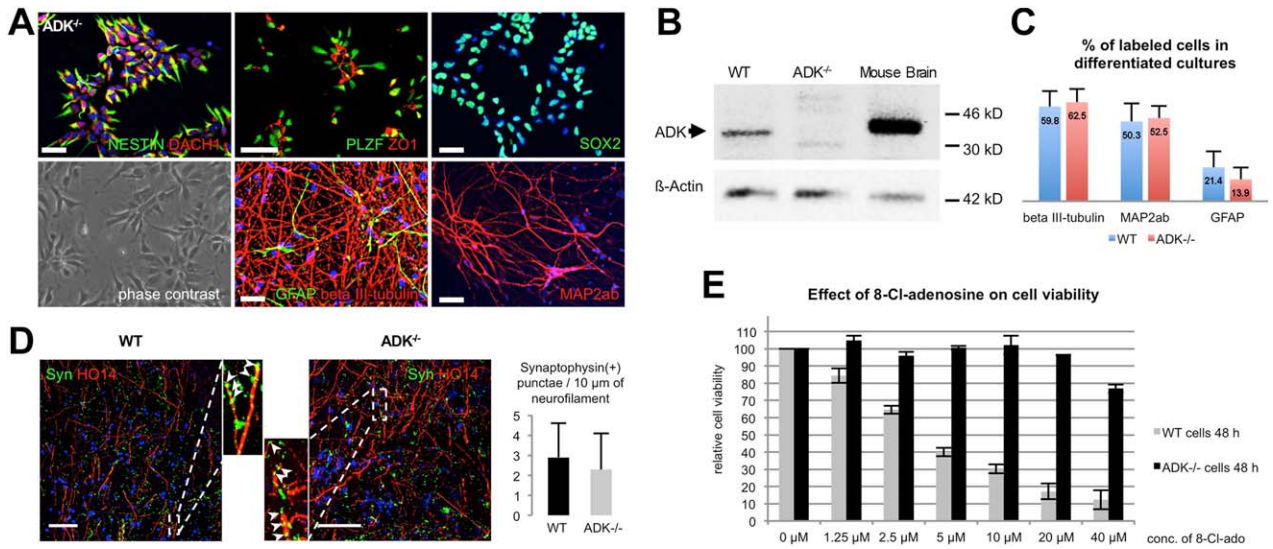

Figure 2. Characterization of ADK-deficient neural stem cells. **(A):** Morphology and marker expression of ADK$^{-/-}$ long-term self-renewing neuroepithelial stem cells were comparable to wild-type cells with rosette-like appearance and the expression of NESTIN, PLZF, SOX2, and polarized ZO-1 expression in the proliferating stage as well as expression of beta III-tubulin, MAP2ab and GFAP upon 5 weeks of differentiation. Scale bars: 50 μm. **(B):** Absence of ADK protein was confirmed by Western blot analysis. Actin served as loading control. Mouse brain protein served as positive control. **(C):** Quantitative analysis reveals comparable numbers of beta III-tubulin-, MAP2ab-, and GFAP-positive cells in differentiated populations derived from wild-type and ADK$^{-/-}$ cells. **(D):** Following transplantation, both populations efficiently differentiated into neurons (detected by a human-specific antibody to neurofilaments HO14). Human synaptophysin-positive punctae were detected in neuronal projection regions (enlarged regions show synaptophysin-positive dots in close vicinity to human neurofilaments marked by arrowheads). No significant difference was detected when we compared the ratio of synaptophysin-positive punctae to the length of human neurofilament-positive fibers, suggesting that wild-type and ADK$^{-/-}$ cells exhibit comparable in vivo differentiation and integration potential (unpaired *t* test, $p = .6705$; scale bars: 50 μm). **(E):** Relative viability of WT or ADK$^{-/-}$ cells after 48 hours exposure to increasing concentrations of 8-Cl-adenosine as assessed by PrestoBlue assay. Only ADK-deficient cells tolerated the additional chemoselection with 8-Cl-Adenosine, while wild-type cells showed pronounced cytotoxicity. Abbreviations: ADK, adenosine kinase; GFAP, glial fibrillary acidic protein; WT, wild-type.

compared to wild-type cells after a 24 hours period (Supporting Information Fig. S6), whereas at earlier time points, the adenosine levels were below the detection levels (data not shown). To increase the sensitivity of adenosine detection, we added erythro-9-(2-hydroxy-3-nonyl)adenine (EHNA), a compound suppressing the decay of adenosine via ADA [30], and extended the time period for media collection. With this modification, we detected a significant increase in the adenosine content in the ADK$^{-/-}$ populations 2 hours following media change to LC-MS/MS cell buffer, which further increased over time (Fig. 3A and Supporting Information Fig. S6). Specifically, adenosine release from ADK$^{-/-}$ lt-NES cells increased from 73.85 ± 3.25 ng (normalized to adenosine content per 100,000 cells) after 2 hours to 456.18 ± 5.73 ng after 24 hours compared to 0.85 ± 1.17 ng and 5.19 ± 0.81 ng in wild-type lt-NES cells, respectively. Following 5 weeks of differentiation, we observed a comparable result with differentiated ADK$^{-/-}$ lt-NES cells releasing 67.66 ± 4.42 ng after 2 hours and 364.27 ± 48.39 ng after 24 hours compared to 0.87 ± 0.09 ng and 0.15 ± 0.23 ng in differentiated wild-type lt-NES cells (Fig. 3A). As differentiated lt-NES cells comprise both, neurons and astrocytes, we investigated the adenosine content of each individual subpopulation. To that end we applied differentiation protocols, which give rise to enriched neuronal or astroglial cell populations. For the generation of enriched neurons, we applied treatment with the gamma-secretase inhibitor N-[N-(3,5-difluorophenacetyl)-L-alanyl]-*S*-phenylglycine *t*-butyl ester (DAPT [31]). Differentiated populations generated this way exhibited 78.9% ± 5.8% beta III-tubulin-positive neurons and only 8.8% ± 3.2% of GFAP expressing cells as well as 12.3% ± 4.7% of cells not stained with either of both antibodies (Fig. 3B). For the generation of an astrocyte-enriched cell population, we used longer differentiation times of 8 weeks and supplementation with fetal calf serum from week 2 to 5 of the differentiation process [24]. Resulting populations contained 88.0% ± 5.1% GFAP-positive astrocytes, 2.8% ± 1.9% beta III-tubulin-positive neurons and 9.3% ± 3.2% cells negative for both markers. We first investigated the expression of ADK and ADA in both cultures. While we found that ADA is expressed only slightly higher in astrocyte-enriched cultures compared to neuron-enriched cultures, expression of ADK was several-fold higher in astrocytic versus neuronal cultures (Fig. 3C). This is in line with previous reports showing that in postnatal mouse brain ADK is substantially higher expressed in astrocytes compared to neurons [32]. Accordingly, we observed lower basal levels of secreted adenosine in astrocyte-enriched compared to neuron-enriched cultures (29.13 ± 19.40 ng in neurons compared to 16.43 ± 10.11 ng in astrocytes). In the knockout situation, secretion of adenosine was strongly increased especially in neuron-enriched cultures (350.04 ± 25.68 ng in neurons compared to 42.37 ± 4.41 ng in astrocyte-enriched cultures; adenosine concentrations all normalized to 100,000 cells per 24 hours, Fig. 3D, left columns). Thus, ADK$^{-/-}$ lt-NES cells and their differentiated progeny robustly secrete adenosine compared to the wild-type controls with lt-NES cell-derived neuronal cells exhibiting the strongest adenosine releasing capacity.

Excitation Induces Adenosine Release from Neuronal Cultures

We previously showed that adenosine-releasing murine embryonic stem cell-derived neural cells are superior to adenosine-releasing non-neuronal baby hamster kidney cells in a rat model

of epileptogenesis [21]. This beneficial effect could be due to several reasons, including better provision of adenosine to the CNS tissue via axonal and dendritic extensions or an activity-dependent release from neuronal cells. If employed as cell-mediated therapy for the treatment of epilepsy, adenosine-releasing cells should ideally be able to deliver adenosine "on

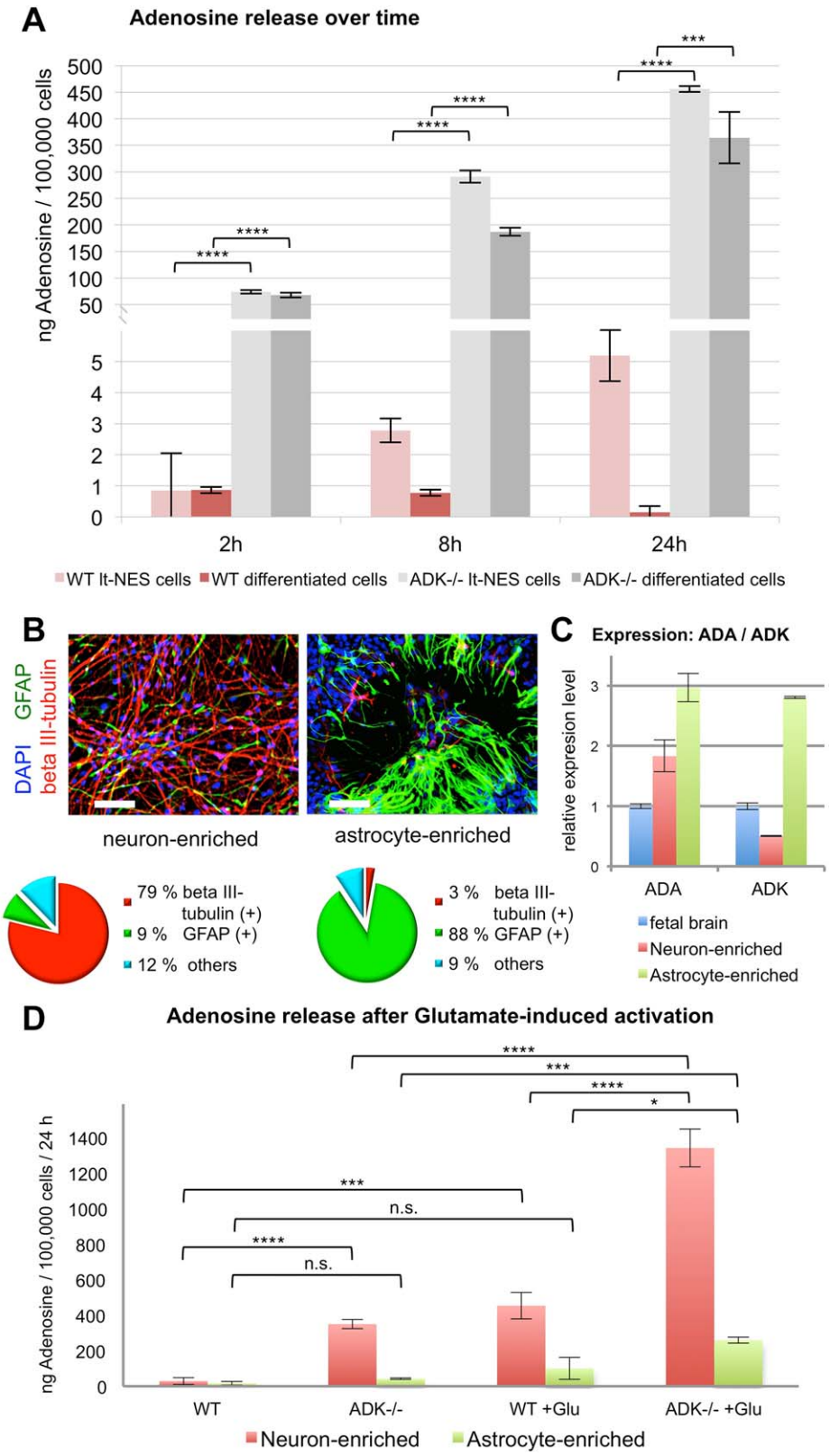

Figure 3.

demand," that is, concomitant to excess neuronal activity during seizures or status epilepticus. In previous studies, we demonstrated that lt-NES cell-derived neurons differentiated for >6 weeks establish functional synaptic connections, show spontaneous synaptic network activity and are responsive to excitatory stimulation by neurotransmitters [22–25]. To test whether release of adenosine from human differentiated ADK$^{-/-}$ neural stem cells could be induced by neuronal excitation, we thus treated differentiated neuron-enriched and astrocyte-enriched ADK$^{-/-}$ and wild-type cultures twice with 100 μM L-glutamate 1 and 8 hours following media change to detection buffer [24]. Following glutamate treatment, levels of secreted adenosine in wild-type cells increased to 100.62 ± 61.85 ng when stimulating astrocytes, and to 453.41 ± 74.14 ng when stimulating neurons with L-glutamate, indicating that L-glutamate stimulation can elicit adenosine secretion from differentiated neural cell populations. This effect was much more pronounced in the ADK$^{-/-}$ cells with values rising to 259.47 ± 26.76 ng in astrocyte-enriched cultures and to 1,342.55 ± 106.55 ng in neuron-enriched cultures, indicating that excitation by neurotransmitter-induced stimulation can increase basal adenosine release nearly by fourfold in these cells (adenosine concentrations all normalized to 100,000 cells per 24 hours, Fig. 3D, right columns). A similar effect could be elicited when stimulating the cultures with NMDA and AMPA, while glutamate-stimulated adenosine release was strongly reduced in the presence of specific inhibitors of AMPA and NMDA receptors, that is, D-APV and 2,3-dihydroxy-6-nitro-7-sulfamoyl-benzo[f]quinoxaline-2,3-dione (NBQX), respectively (Supporting Information Fig. S7). To exclude that this increase of adenosine in the supernatant is due to toxicity exerted by glutamate treatment and potential lysis of the cells, we measured cell viability of the cells 8 hours after stimulation with increasing glutamate concentrations. This analysis revealed no obvious glutamate-induced reduction of cell viability under the glutamate exposure conditions used in this study (Supporting Information Fig. S8). Together these data suggest that the increased adenosine release observed after glutamate stimulation is due to excitation of the cultures and not to unspecific modes of action or general toxicity.

Discussion

The role of adenosine as a potential therapeutic drug for the treatment of various pathological conditions of the brain such as epilepsy, stroke, depression, or pain has compelled researchers to search for potential systems to safely deliver adenosine to the brain. Cells deficient in the metabolizing enzyme ADK have proved to be an attractive therapeutic tool for the local delivery of adenosine. Initial experiments applied non-neural cells, which resulted in strong but temporally limited antiepileptic activity [18–20]. Using mouse ADK-deficient embryonic stem cell-derived neural cell populations, we demonstrated (a) strongly enhanced levels of secreted adenosine compared to cells derived from wild-type controls [33], (b) short-term protection of murine brains against experimental epileptogenesis upon grafting encapsulated ADK-deficient cells into the ventricles of rats subjected to kindling [34], and (c) efficient suppression of kindling-induced epileptogenesis and seizure severity upon direct transplantation of ADK$^{-/-}$ cells into the hippocampus of rats [21]. However, translation of these findings to human cells was, for a long time, complicated by the fact that homologous recombination in human cells proved to be highly inefficient [35]. With the recent advent of genome editing technologies such as ZFNs [36], transcription activator-like effector nucleases [37], and CRISPR-Cas/RNA-guided nucleases [38], gene editing has become broadly applicable to human cells. Typically, these techniques are applied to human pluripotent stem cells, which are then used to derive defined somatic cell types required for the individual application. Considering that our recently described population of lt-NES cells exhibits highly stable long-term proliferation and differentiation capacity, we became interested in whether targeting of the ADK locus could be directly accomplished in these human neural cells. To that end we used a ZFN-based gene disruption approach, that resulted in the bi-allelic knockout of the ADK gene in human lt-NES cells, thereby providing the first reported human ADK-deficient cell population.

Targeting stable tissue-specific precursors rather than their parental pluripotent stem cells has a number of advantages. First, time requirements are significantly reduced because genetic modification is directly conducted in the target cell population. Second, this approach bypasses the risk that the genetic modification itself interferes with the maintenance and proper differentiation of the pluripotent ancestral cells. Finally, the resulting phenotype can be directly assessed in the target cell populations. In addition, lt-NES cells provide advantages with respect to potential biomedical applications in that they (a) are highly homogeneous and devoid of any remaining pluripotent cells with potential teratoma-initiating capacity [22], (b) consistently give rise to high numbers of neurons capable of integrating into synaptic circuits in vivo [22] and (c) can be generated from any pluripotent cell source including patient-specific iPSCs [24] and haplotype-matched cells from cell banks, thereby providing prospects for avoiding the risk of rejection and the need for immunosuppression.

Targeting the *ADK* locus was largely facilitated by the possibility to use chemical selection. For enrichment of correctly targeted cells, no further genetic modification was necessary, as the enzyme-specific antimetabolites 8-chloro-adenosine and 8-chloro-cAMP could be used for selection. We confirmed the functional disruption of the *ADK* gene by genome sequencing and Western blotting. One prerequisite for a therapeutic application of in vitro

Figure 3. ADK$^{-/-}$ cell populations exhibit increased adenosine release. **(A):** Comparison of adenosine release (in ng per 100,000 cells) into the culture media by wild-type lt-NES cells, ADK$^{-/-}$ lt-NES cells and their differentiated progeny at 2, 8, and 24 hours. **(B):** Astrocyte- or neuron-enriched cultures of ADK$^{-/-}$ cells after differentiation stained for beta III-tubulin (neuronal marker; 5 weeks of differentiation) and GFAP (astrocytic marker; 8 weeks of differentiation). Pie charts depict the composition of each culture (neuronal cultures: 78.9% ± 5.8% neurons, 8.8% ± 3.2% astrocytes, 12.3% ± 4.7% other cells; astrocytic cultures: 2.8% ± 1.9% neurons, 88.0% ± 5.1% astrocytes, 9.3% ± 3.2% other cells). **(C):** Quantitative RT-PCR analysis of ADA and ADK expression in neuron- and astrocyte-enriched cultures, compared to human fetal brain RNA (set to 1). **(D):** Adenosine levels in supernatants of neuronal and astrocytic cultures of wild-type and ADK$^{-/-}$ cells were measured with or without stimulation with glutamate. Glutamate generally induced an increase in adenosine efflux, which was particularly prominent in ADK$^{-/-}$ neuronal cultures. Scale bars: 100 μm. Statistical analysis: *, $p < .05$; **, $p < .01$; ***, $p < .001$; ****, $p < .0001$. Abbreviations: ADA, adenosine deaminase; ADK, adenosine kinase; DAPI, 4′,6-diamidino-2-phenylindole; GFAP, glial fibrillary acidic protein; lt-NES, long-term self-renewing neuroepithelial stem; RT-PCR, reverse transcription polymerase chain reaction; WT, wild-type.

engineered cells is the necessity to guarantee genomic integrity and robust differentiation potential. Using high-resolution whole genome SNP karyotyping, we show that ADK-deficient human neural stem cells can be generated without overt karyotypic alterations. These cells show growth properties comparable to their nonmodified counterpart and maintain their ability to generate neurons and glia over several passages. However, it is important to note that the resolution of our SNP analyses is not sufficient to entirely exclude off-target alterations induced by the genetic manipulation or the selection process. While our study provides a prove of principle for the generation of an ADK-deficient human neural cell population, a potential clinical application of such cells would require a much more detailed assessment of genetic integrity including, for example, whole genome sequencing.

When addressing adenosine levels in the culture supernatant of engineered lt-NES cells and their differentiated progeny by HPLC-MS/MS we could confirm a robust induced adenosine releasing capacity in both populations, ranging to up to over 400 ng/ml per 100,000 cells within 24 hours. Such concentrations should be sufficient to substantially counteract epileptic activity as previous studies with mouse-derived stem cells showed that adenosine release between 160 and 330 ng adenosine per 100,000 cells per 24 hours was sufficient to fulfill this task, even though detection methods for the amount of adenosine release differ between the studies [18, 19, 34]. Adenosine release could be further triggered by glutamate-induced excitation with adenosine levels reaching up to 1,700 ng/ml per 100,000 cells per 24 hours, suggesting that once integrated into the host brain circuitry, ADK-deficient neurons might be able to directly respond to increased seizure-associated neuronal activity by releasing adenosine, thereby inhibiting further tissue damage and the process of epileptogenesis [40]. Given the fact that lt-NES cells mainly differentiate into neurons with a GABAergic neurotransmitter phenotype, it is tempting to speculate that ADK-deficient lt-NES cell-derived neurons might elicit antiepileptic activity not only by release of adenosine but synergistically via GABA-mediated inhibition of neuronal networks as previously shown in a murine pilocarpine model [41, 42].

Notwithstanding these biomedical prospects, extensive preclinical studies will be required to determine whether and to what extent adenosine releasing human neural cell populations can be used as the basis for a cell-based therapy. In this context, it is important to note that ADK expression differs in the young and the mature brain with preferential expression in neurons and astrocytes in the developing and mature brain, respectively [32]. This developmental shift of ADK expression suggests distinct roles of this enzyme during brain development. Nevertheless, the results of several studies support the notion that human neurons in the adult brain exhibit low expression of ADK [43, 44]. Interestingly, it has been reported that expression of ADK is upregulated in the context of CNS lesions and that this reactive increase is associated with a local adenosine deficiency in reactively altered brain tissue [45]. Such an adenosine deficiency could be counteracted by engrafted ADK-deficient cells, which themselves would be "protected" against a reactive upregulation of ADK.

In addition to the potential treatment of epilepsy and epileptogenesis where adenosine might not only act as an acute antiepileptic drug but might also prevent upregulation of ADK in the surrounding tissue via activation of A_1-receptors in local astrocytic populations [40], exploitation of neuroprotective effects of such cells in cerebral hypoxia could provide another attractive therapeutic avenue. In line with this idea, ADK-deficient embryonic stem cell-derived glial progenitors were demonstrated to significantly reduce the infarcted area and improve neurological scores in a model of ischemic brain injury [46]. In multiple sclerosis, adenosine has been described as a mediator promoting oligodendrocyte differentiation and myelination [39]. In chronic and neuropathic pain, adenosine was shown to exhibit potent analgesic actions [47], and intrathecal implants of adenosine-releasing neural cell populations might qualify as therapeutic modality for pain control. The $ADK^{-/-}$ neural stem cells described in this study should provide a useful asset to explore these approaches using a highly standardized human cell system.

Conclusion

This study generated human neuroepithelial stem cells (lt-NES cells) deficient for ADK, the most important cellular metabolizing enzyme of adenosine. The purine nucleoside adenosine has been described to have extensive neuroprotective properties under various pathological conditions of the brain and can counteract overshooting neuronal activity. The resulting cells can be efficiently differentiated into neurons and astrocytes in vitro and in vivo and exhibit elevated adenosine releasing capacities. Secretion of adenosine from neurons can be triggered by excitation, providing the basis for exploiting ADK-deficient neurons as an attractive therapeutic tool for local "on-demand" delivery of adenosine in epilepsy and other neurological disorders.

Acknowledgments

The human hESC-derived lt-NES cell line was previously generated from the hESC line I3 (hES-1), which was originally provided by Joseph Itskovitz-Eldor (Technion, Israel Institute of Technology, Haifa, Israel). We thank Virginia Lee for providing the HO14 antibody. Single nucleotide polymorphism analysis was performed by the Institute of Human Genetics (LIFE & BRAIN Center). This work was supported by the Deutsche Forschungsgemeinschaft (SFB-TR3–05/D2) and the Hertie Foundation.

Author Contributions

D.P.: conception and design, collection and/or assembly of data, data analysis and interpretation, manuscript writing; J.D., M.S., R.W., J.A.S., and J.L.: collection and/or assembly of data, data analysis and interpretation; A.T., D.E.P., P.D.G., and A.R.: collection and/or assembly of data, manuscript writing; C.E.M.: data analysis and interpretation, manuscript writing; P.K.: conception and design, collection and/or assembly of data, data analysis and interpretation, manuscript writing, final approval of manuscript; O.B.: conception and design, financial support, data analysis and interpretation, manuscript writing, final approval of manuscript.

Disclosure of Potential Conflicts of Interest

O.B. is a cofounder and has stock in LIFE & BRAIN GmbH. A.R., A.T., D.E.P., and P.D.G. are current or former employees of Sangamo Therapeutics, Inc. The other authors indicated no potential conflicts of interest.

References

1 Jacobson KA. Introduction to adenosine receptors as therapeutic targets. In: Wilson CN, Mustafa SJ, eds. Adenosine Receptors in Health and Disease. 1st ed. Berlin, Germany: Springer-Verlag, 2009:1–24.

2 Karmouty-Quintana H, Xia Y, Blackburn M. Adenosine signaling during acute and chronic disease states. J Mol Med 2013;91: 173–181.

3 Fredholm BB. Adenosine, an endogenous distress signal, modulates tissue damage and repair. Cell Death Differ 2007;14:1315–1323.

4 Berman RF, Fredholm BB, Aden U et al. Evidence for increased dorsal hippocampal adenosine release and metabolism during pharmacologically induced seizures in rats. Brain Res 2000;872:44–53.

5 Klaft ZJ, Hollnagel JO, Salar S et al. Adenosine A1 receptor-mediated suppression of carbamazepine-resistant seizure-like events in human neocortical slices. Epilepsia 2016;57:746–756.

6 Boison D. Adenosine dysfunction in epilepsy. Glia 2012;60:1234–1243.

7 Masino SA, Kawamura M Jr., Ruskin DN. Adenosine receptors and epilepsy: Current evidence and future potential. Int Rev Neurobiol 2014;119:233–255.

8 Boison D, Stewart KA. Therapeutic epilepsy research: From pharmacological rationale to focal adenosine augmentation. Biochem Pharmacol 2009;78:1428–1437.

9 Dunwiddie TV. Adenosine and suppression of seizures. Adv Neurol 1999;79:1001–1010.

10 Pagonopoulou O, Efthimiadou A, Asimakopoulos B et al. Modulatory role of adenosine and its receptors in epilepsy: Possible therapeutic approaches. Neurosci Res 2006;56:14–20.

11 Van Dycke A, Raedt R, Dauwe I et al. Continuous local intrahippocampal delivery of adenosine reduces seizure frequency in rats with spontaneous seizures. Epilepsia 2010;51: 1721–1728.

12 Szybala C, Pritchard EM, Lusardi TA et al. Antiepileptic effects of silk-polymer based adenosine release in kindled rats. Exp Neurol 2009;219:126–135.

13 Arch JR, Newsholme EA. Activities and some properties of 5'-nucleotidase, adenosine kinase and adenosine deaminase in tissues from vertebrates and invertebrates in relation to the control of the concentration and the physiological role of adenosine. Biochem J 1978;174:965–977.

14 Boison D. Adenosine-based cell therapy approaches for pharmacoresistant epilepsies. Neurodegener Dis 2007;4:28–33.

15 Jennings LL, Hao C, Cabrita MA et al. Distinct regional distribution of human equilibrative nucleoside transporter proteins 1 and 2 (hENT1 and hENT2) in the central nervous system. Neuropharmacology 2001;40:722–731.

16 Baldwin SA, Beal PR, Yao SY et al. The equilibrative nucleoside transporter family, SLC29. Pflugers Arch 2004;447:735–743.

17 Baldwin SA, Mackey JR, Cass CE et al. Nucleoside transporters: Molecular biology and implications for therapeutic development. Mol Med Today 1999;5:216–224.

18 Huber A, Padrun V, Déglon N et al. Grafts of adenosine-releasing cells suppress seizures in kindling epilepsy. Proc Natl Acad Sci USA 2001;98:7611–7616.

19 Güttinger M, Padrun V, Pralong WF et al. Seizure suppression and lack of adenosine A1 receptor desensitization after focal long-term delivery of adenosine by encapsulated myoblasts. Exp Neurol 2005;193:53–64.

20 Ren G, Li T, Lan JQ et al. Lentiviral RNAi-induced downregulation of adenosine kinase in human mesenchymal stem cell grafts: A novel perspective for seizure control. Exp Neurol 2007;208:26–37.

21 Li T, Steinbeck JA, Lusardi T et al. Suppression of kindling epileptogenesis by adenosine releasing stem cell-derived brain implants. Brain 2007;130:1276–1288.

22 Koch P, Opitz T, Steinbeck JA et al. A rosette-type, self-renewing human ES cell-derived neural stem cell with potential for in vitro instruction and synaptic integration. Proc Natl Acad Sci USA 2009;106:3225–3230.

23 Falk A, Koch P, Kesavan J et al. Capture of neuroepithelial-like stem cells from pluripotent stem cells provides a versatile system for in vitro production of human neurons. PLoS One 2012;7:e29597.

24 Koch P, Breuer P, Peitz M et al. Excitation-induced ataxin-3 aggregation in neurons from patients with Machado-Joseph disease. Nature 2011;480:543–546.

25 Steinbeck JA, Koch P, Derouiche A et al. Human embryonic stem cell-derived neurons establish region-specific, long-range projections in the adult brain. Cell Mol Life Sci 2012; 69:461–470.

26 Urnov FD, Miller JC, Lee YL et al. Highly efficient endogenous human gene correction using designed zinc-finger nucleases. Nature 2005;435:646–651.

27 Bozas A, Beumer KJ, Trautman JK et al. Genetic analysis of zinc-finger nuclease-induced gene targeting in Drosophila. Genetics 2009;182:641–651.

28 Gandhi V, Ayres M, Halgren RG et al. 8-chloro-cAMP and 8-chloro-adenosine act by the same mechanism in multiple myeloma cells. Cancer Res 2001;61:5474–5479.

29 Siemen H, Nix M, Endl E et al. Nucleofection of human embryonic stem cells. Stem Cells Dev 2005;14:378–383.

30 Schaeffer HJ, Schwender CF. Enzyme inhibitors. 26. Bridging hydrophobic and hydrophilic regions on adenosine deaminase with some 9-(2-hydroxy-3-alkyl)adenines. J Med Chem 1974;17:6–8.

31 Borghese L, Dolezalova D, Opitz T et al. Inhibition of notch signaling in human embryonic stem cell-derived neural stem cells delays G1/S phase transition and accelerates neuronal differentiation in vitro and in vivo. Stem Cells 2010;28:955–964.

32 Studer FE, Fedele DE, Marowsky A et al. Shift of adenosine kinase expression from neurons to astrocytes during postnatal development suggests dual functionality of the enzyme. Neuroscience 2006;142:125–137.

33 Fedele DE, Koch P, Scheurer L et al. Engineering embryonic stem cell derived glia for adenosine delivery. Neurosci Lett 2004; 370:160–165.

34 Güttinger M, Fedele DE, Koch P et al. Suppression of kindled seizures by paracrine adenosine release from stem cell-derived brain implants. Epilepsia 2005;46:1162–1169.

35 Zwaka TP, Thomson JA. Homologous recombination in human embryonic stem cells. Nat Biotechnol 2003;21:319–321.

36 Bibikova M, Carroll D, Segal DJ et al. Stimulation of homologous recombination through targeted cleavage by chimeric nucleases. Mol Cell Biol 2001;21:289–297.

37 Christian M, Cermak T, Doyle EL et al. Targeting DNA double-strand breaks with TAL effector nucleases. Genetics 2010;186:757–761.

38 Jinek M, East A, Cheng A et al. RNA-programmed genome editing in human cells. Elife 2013;2:e00471.

39 Tsutsui S, Schnermann J, Noorbakhsh F et al. A1 adenosine receptor upregulation and activation attenuates neuroinflammation and demyelination in a model of multiple sclerosis. J Neurosci 2004;24:1521–1529.

40 Boison D. Role of adenosine in status epilepticus: A potential new target? Epilepsia 2013;54:20–22.

41 Cunningham M, Cho JH, Leung A et al. hPSC-derived maturing GABAergic interneurons ameliorate seizures and abnormal behavior in epileptic mice. Cell Stem Cell 2014;15:559–573.

42 Hunt RF, Girskis KM, Rubenstein JL et al. GABA progenitors grafted into the adult epileptic brain control seizures and abnormal behavior. Nat Neurosci 2013;16:692–697.

43 Luan G, Gao Q, Zhai F et al. Adenosine kinase expression in cortical dysplasia with balloon cells: Analysis of developmental lineage of cell types. J Neuropathol Exp Neurol 2015;74:132–147.

44 Uhlén M, Fagerberg L, Hallström BM et al. Proteomics. Tissue-based map of the human proteome. Science 2015;347:1260419.

45 Boison D. The adenosine kinase hypothesis of epileptogenesis. Prog Neurobiol 2008; 84:249–262.

46 Pignataro G, Studer FE, Wilz A et al. Neuroprotection in ischemic mouse brain induced by stem cell-derived brain implants. J Cereb Blood Flow Metab 2007;27:919–927.

47 Lynch ME, Clark AJ, Sawynok J. Intravenous adenosine alleviates neuropathic pain: A double blind placebo controlled crossover trial using an enriched enrolment design. Pain 2003;103:111–117.

See www.StemCellsTM.com for supporting information available online.